Aberration corrected STEM of iron rhodium nanoislands

M J McLaren[1], F S Hage[2], M Loving[3], Q M Ramasse[2], L H Lewis[3], C H Marrows[4], R M D Brydson[1]

[1]Institute of Materials Research, SPEME, University of Leeds, LS2 9JT, UK
[2]SuperSTEM Laboratory, SciTech Daresbury Campus, Daresbury WA4 4AD, UK
[3]Department of Chemical Engineering, Northeastern University, Boston, MA 02115, USA
[4]School of Physics and Astronomy, University of Leeds, LS2 9JT, UK

E-mail: py06mjm@leeds.ac.uk

Abstract. Iron-rhodium (FeRh) nanoislands of equiatomic composition have been analysed using scanning transmission electron microscopy (STEM) electron energy loss spectroscopy(EELS) and high angle annular dark field (HAADF) techniques. Previous magnetometry results have lead to a hypothesis that at room temperature the core of the islands are antiferromagnetic while the shell has a small ferromagnetic signal. The causes of this effect are most likely to be a difference in composition at the edges or a strain on the island that stretches the lattice and forces the ferromagnetic transition. The results find, at the film-substrate interface, an iron-rich layer ~ 5 Å thick that could play a key role in affecting the magnetostructural transition around the interfacial region and account for the room temperature ferromagnetism.

1. Introduction

Iron-rhodium (FeRh) alloys exhibit an unusual magnetostructural transition, making them an interesting area of research. When in an approximately equiatomic state ($Fe_{48}Rh_{52}$ to $Fe_{56}Rh_{44}$), the alloy is in an ordered α' state and arranged in a CsCl structure[1]. At room temperature, FeRh is antiferromagnetic, but makes a first-order phase transition upon heating to a ferromagnetic (FM) state at $\sim$350 K[2].

The transition also has a uniform 1% increase[3] in unit cell lattice volume when heating to the ferromagnetic phase, which correlates to a lattice parameter increase of 2.987 Å to 2.997 Å[1] (a change of 0.3%). Other characteristics associated with the phase transition include an increase in entropy[4] and drop in resistivity[5] when changing to the FM phase as well as a $\sim$10 K temperature hysteresis[6] in bulk. The properties of the phase change can be controlled by altering the structure of the FeRh *via* multiple methods, including ion beam irradiation[7] and chemical doping with various elements[8]. One other technique of altering the magnetic transition discussed here is growing FeRh epitaxially onto a substrate with a small lattice mismatch. The epitaxial growth causes a compressive or tensile strain on the FeRh lattice (depending on whether the lattice parameter of the substrate is larger or smaller than that of FeRh), thereby causing an increase in the transition temperature with a compressed lattice and vice versa[9].

Due to the magnetic phase change and its ability to be tuned to specific temperatures, FeRh has potential uses for spin valves in magnetic data storage or microelectromechanical systems[10].

There is an interest in using electron microscopy to fully characterise the FeRh system when epitaxially grown onto a substrate. Much work has been done on the magnetic properties of the transition but little has been done to relate these properties to the nanostructure of the thin films. In particular, there is much interest in the regions surrounding the interfaces because of the potential changes in structure and magnetism located here. In this paper we discuss FeRh samples that have grown in an island-like structure. These are found to have a ferromagnetic signal in the nominally AFM phase with close contact between the two regions as determined by SQUID magnetometry[11]. It is hypothesised that each nanoisland has an AFM core with a FM shell that surrounds it. The reason for this phase coexistence is unknown but could either be as a result of strain, a change in composition around the shell or a combination of the two.

2. Experimental

The FeRh film was grown by sputtering onto a magnesium oxide (MgO) substrate, deposited from a single target. The samples were annealed at 700 °C then capped in-situ with a 20-30 Å layer of Al using methods that have been described in detail elsewhere[11][12].

For observation in the TEM, the sample was prepared into a cross section by focused ion beam (FIB) using a FEI Nova 200 NanoLab dual beam FIB with a Ga ion source. A layer of platinum was deposited over the area of interest to protect from damage. A 30 kV beam at 20 nA excavated both sides of the region to a depth of 5 μm. The sample was then thinned further using a beam current of 100 pA. The sample was lifted out in-situ by welding to a micromanipulator and moved to a TEM sample holder.

The sample was characterised in the Nion UltraSTEM100 operated at 100 kV using high angle annular dark field (HAADF) scanning TEM (STEM) and STEM-electron energy loss spectroscopy (EELS) techniques with the EELS data denoised in DigitalMicrograph using principle component analysi[13].

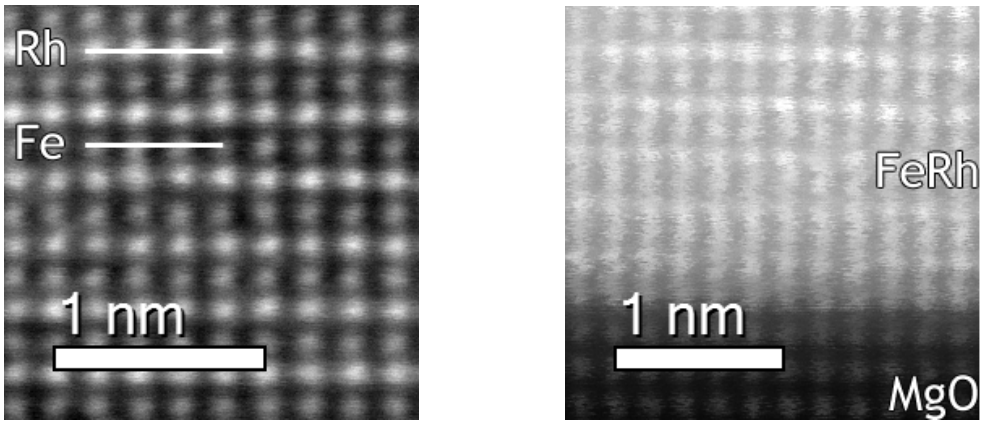

Figure 1. HAADF-STEM images showing the structure at the centre of the island averaged from an image stack (left) and at the interface with MgO (right). With both images, the expected CsCl structure can be seen viewing along the (110) zone axis, with alternating rows of Fe and Rh (dark and bright respectively, due to the differences in their atomic number), however any minor changes in FeRh composition are not observable through HAADF alone.

3. Results and Discussion

Figure 1 shows HAADF-STEM images comparing the structure in the middle of an island (a) and at the FeRh-MgO interface (b). The difference in contrast between Fe (dark) and Rh (bright) is visible due to the large difference in atomic number. Viewing the structure along the

(110) axis, the CsCl structure can be seen. X-ray diffraction techniques are generally applied to determine a chemical order factor, S, to determine the chemical order of the sample[12]. This value is typically ~ 0.8 for FeRh films grown using the described method, meaning 10% of Fe will be located on the Rh sites and vice versa. Directly detecting this chemical disorder in the HAADF of this scale is difficult in these images so it is unlikely that, unless the displacement of Fe and Rh is significant, a contrast change will be noticeable.

Figure 2a shows EELS maps for Fe $L_{2,3}$, Rh $M_{4,5}$ and O K edges at the FeRh interface with MgO. The intensities of Fe and Rh alternate with each row with a terminating Fe layer at the interface with MgO. This initial observation fits well with the expected crystal structure of FeRh. The oxygen signal drops significantly across the interface, showing no discernible diffusion into the FeRh. For the first two rows of Fe, the signal is overwhelmingly strong relative to the other rows. The first Rh row is extremely weak in comparison, suggesting that the Fe content in this area is higher than Rh. It is known that rhodium oxides do not readily occur due to their small free energies of formation[14]. In comparison, iron oxides have a greater tendency to form[15]. The fine structure data in figure 2b shows an O-K pre-peak indicative of a transition metal oxide bond[16].

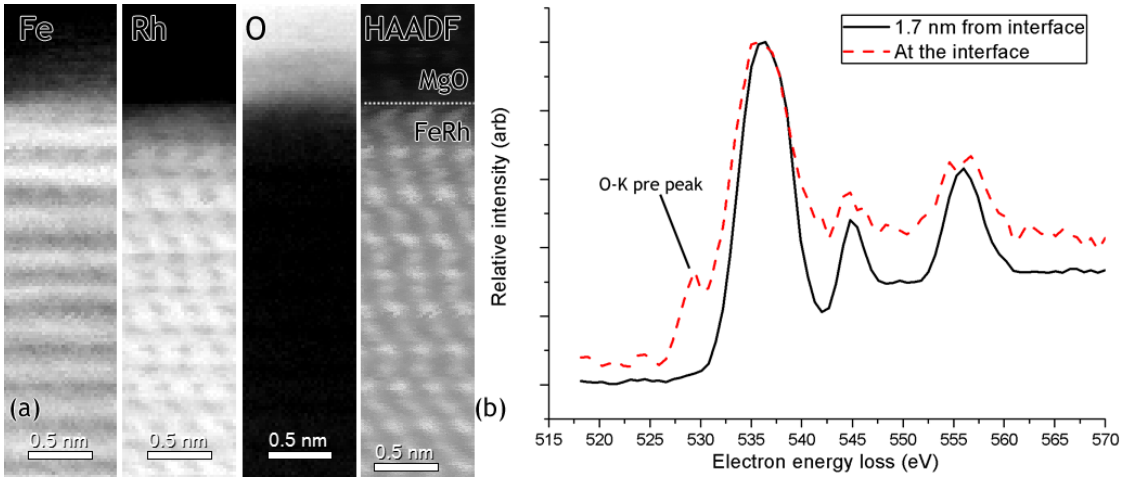

Figure 2. (a) STEM-EELS maps acquired at the FeRh-MgO interface, with maps for iron $L_{2,3}$, rhodium $M_{4,5}$ and oxygen K edges. A HAADF image of the same region is provided for comparison, with a dotted line indicating the FeRh-MgO interface. There is a variation in intensity for the first two Fe rows, which appear brighter than the other Fe layers. The distortion in the FeRh lattice is believed to be as a result of interaction between the beam and the magnetic sample. (b) Typical O-K spectra along and 1.7 nm from the interface into the MgO, showing the difference in fine structure. There is an obvious pre-peak on the interfacial spectrum indicating a transition metal oxide bond which, combined with the EELS maps, confirms an Fe terminating layer.

Taking 20 pixel integrated line profiles of the EELS maps obtained in figure 2a, the interfacial changes can be seen much more clearly. Figure 3 plots the relative intensities of the profiles with distance, with a comparison to the HAADF of the same area. The change in intensity for the first three layers of FeRh atoms is very clear, with the first two Fe layers appearing stronger and the first Rh layer showing a diminished peak. This result shows clearly that there is a relative change in composition at the interface that results in a narrow (~ 5 Å) Fe-rich band relative to the surrounding area. As these islands are expected to be equiatomic, there should be diffusion

of Rh from this Fe-rich region to elsewhere in the island. However, the small compositional variations expected (e.g. $Fe_{48}Rh_{52}$) were not immediately detectable with the equipment used.

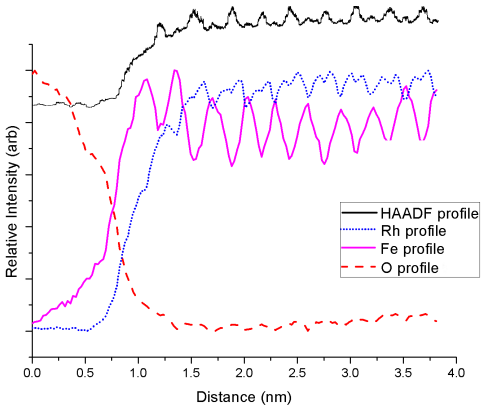

Figure 3. Line profiles taken from the above EELS maps, showing the relative change of Fe, Rh and O across the FeRh-MgO interface. The first two rows of Fe atoms have a noticeably stronger signal relative to the rest of the atoms and the first Rh layer (in between the two Fe rows) is diminished in comparison to the remaining layers. The HAADF profile for the same area is offset above. The intensity change at the interface cannot be seen on the HAADF.

4. Conclusions

The interfacial EELS maps show that, in general, the FeRh crystal is layered as expected with alternating Fe and Rh layers with a strong Fe signal detected for the first two rows of Fe atoms. Closer examination using line profiles shows very clearly that the Rh concentration is significantly lower in the first nominally Rh layer and the increased Fe signal is the result of an Fe-rich area in the first ~ 5 Å of the FeRh film at the interface with the substrate. An Fe-rich band along the interface would likely be ferromagnetic as expected from the FeRh phase diagram[1] and provide an explanation for ferromagnetic signal in the nominally antiferromagnetic phase[17]. A Rh-rich region, while not seen, is still quite likely as the FeRh is expected to be equiatomic and diffusion of Fe into the interface would result in displaced Rh. Further investigation with more quantitative analysis could confirm the diffusion of Rh to nearby areas and further investigate the role of composition and interdiffusion on the magnetic transition.

Acknowledgments

This grant has been supported by EPSRC grants EP/G065640/1, EP/F056311/1 and the National Science Foundation grant DMR-0908767.

References

[1] Swartzendruber L J, 1984 Bulletin of Alloy Phase Diagrams 5 45662
[2] Kouvel J S and Hartelius C C, 1962 *J. Appl. Phys.* **33** 1343
[3] Khan M J, 1979 *Phys. F: Metal Phys.* **9** 457
[4] Annaorazov M P, Nikitin S A, Tyurin A L, Asatryan K A, and Dovletov A K,h 1996 *J. App. Phys.* **79** 3
[5] Kouvel J S 1966 *J. App. Phys.* **37** 1257
[6] Ibarra M and Algarabel P, 1994 Phys. Rev. B 50 4196
[7] Aikoh K, Kosugi S, Matsui T and Iwase A, 2011 *J. App. Phys.* **109** 07E311
[8] Schinkel C, Hartog R, and Hochstenbach F, 1974 *J. Phys. F: Metal Phys.* **4** 1412
[9] Maat S, Thiele J and Fullerton E, 2005 *Phys. Rev. B* **72** 21
[10] Thiele J ,Maat S and Fullerton E, 2003 *Appl. Phys. Let.* **82** 17
[11] Loving M et al, 2013 *J. Phys. D* **46** 16
[12] Le Graet C et al, 2013 *J. Vis. Exp.* **in press**
[13] M. Watanabe et al, 2007 *Microsc. Microanal.* **13** 1264. MSA plugin is available from www.hremresearch.com
[14] Jacob K T, Prusty D 2010 *J. Alloys Compd.* **507**
[15] Ragone D 1994 *Thermodynamics of Materials* (Wiley)
[16] Cakvert C C, Brown A, Brydson R 2005 *J. Electron. Spectrosc. Relat. Phenom.* **143**
[17] Fan R et al, 2010 *Phys. Rev. B* **82** 2-6 184418